Published in final edited form as:
*Hum Brain Mapp*. 2011 August ; 32(8): 1260–1276. doi:10.1002/hbm.21106.

# Sequential Temporo-Fronto-Temporal Activation During Monitoring of the Auditory Environment for Temporal Patterns

**Eric Halgren**, **Jason Sherfey**, **Andrei Irimia**, **Anders M. Dale**, and **Ksenija Marinkovic**
Multimodal Imaging Laboratory, Department of Radiology University of California at San Diego

## Abstract

Subjects detected rarely-occurring shifts between two simple tone-patterns, in a paradigm that dissociated the effects of rarity from those of pitch, habituation, and attention. Whole-head magnetoencephalography suggested that rare attended pattern-shifts evoked activity first in the superior temporal plane (STP, peak ~100 ms), then superior temporal sulcus (STS, peak ~130 ms), then posteroventral prefrontal (pvpF, peak ~230 ms), and anterior temporal cortices (aT, peak ~370 ms). Activity was more prominent in the right hemisphere. After subtracting the effects of non-shift tones (balanced for pitch and habituation status), weak but consistent differential effects of pattern-shifts began in aT at 90–130 ms, spread to STS and STP at ~130 ms, then pvpF, and finally returned to aT. Cingulate activity resembled prefrontal. Responses to pattern shifts were greatly attenuated when the same stimuli were ignored, suggesting that the initial superior temporal activity reflected an attention-related Mismatch Negativity. The prefrontal activity at ~230 ms corresponded in latency and task correlates with simultaneously recorded event-related potential **components** N2b and P3a; the subsequent temporal activity corresponded to the P3b. These results were confirmed in sensors specific for frontal or temporal cortex, and thus are independent of the inverse method used. Overall, these results suggest that auditory working memory for temporal patterns begins with detection of the pattern change by an interaction of anterior and superior temporal structures, followed by identification of the event and its consequences led by posteroventral prefrontal and cingulate cortices, and finally, definitive encoding of the event in anterior temporal areas.

### Keywords

music; hippocampal formation; parahippocampal gyrus; auditory cortex; attention; Heschl's gyrus; magnetoencephalography; temporal lobe; prefrontal cortex; cingulate gyrus; insula; operculum; MEG; mismatch negativity; MMN; N2; N200; P300; P3; P3a; human; habituation

## Introduction

Variations in the auditory environment evoke a characteristic set of event-related brain potentials (ERPs) at the scalp. Small deviations from a constant stream of tones evoke pre-attentively a `mismatch negativity' (MMN) (Naatanen 1992). When the stimulus change is sufficient to demand attention, then additional processes embodied in the ERP component termed `P3a' are invoked (Squires, et al. 1975), as a larval form of the orienting response (Marinkovic, et al. 2001). When the auditory stream is explicitly attended, and a behavioral target is identified, the supramodal `N2b-P3b' is emitted (Donchin, et al. 1983).

Please address correspondence to: Eric Halgren, Ph.D. Mail code 0841, UCSD La Jolla, CA 92093-0841 Phone: (858) 822-0762; Fax: (858) 534-1078 ehalgren@ucsd.edu.

A variety of methods have been used to identify the neural substrates of these ERP components. Imaging of hemodynamic increases with PET or fMRI have identified a circuit that is involved in auditory pattern processing- centered in the posterior superior temporal plane (pSTP), but interacting with prefrontal cortex for ongoing context (Zatorre 2001). Hemodynamic studies also suggest that an extended cortical network is activated by deviant auditory stimuli (Linden 2005). However, the sequence of involvement of these structures, and their relation to different scalp ERP components (e.g., MMN vs P3a vs P3b) cannot be determined with hemodynamic measures because of their lack of temporal resolution. Lesions of the postero-superior temporal lobe have been found to suppress the P3 to auditory deviants (Knight, et al. 1988). This decrease is bilateral even though the lesions are unilateral, suggesting that they may be indexing a necessary antecedent process rather than the generator itself (Halgren 2008).

A reasonable candidate for this antecedent process would be the earliest physiological response to deviant auditory stimuli, the MMN. The MMN has a magnetoencephalographic (MEG) counterpart, often termed the MMF (mismatch field). The field-patterns of both the MMN and the MMF correspond well to that expected for a generator in the pSTP (Giard, et al. 1990; Hari, et al. 1984; Jaaskelainen, et al. 2004; Scherg and VonCramon 1985). However, the same scalp topography can result from different intracranial generators. Unambiguous evidence for local generation of the MMN in the pSTP has been provided by intracranial recordings in humans (Halgren, et al. 1995a; Kropotov, et al. 2000; Kropotov, et al. 1995; Rosburg, et al. 2005), monkeys (Javitt, et al. 1994), and cats (Csepe, et al. 1987; Pincze, et al. 2002). These data do not rule out other MMN generators. Furthermore, the stimuli that signalled deviance from background were also subject to frequency-specific dishabituation (see fig 1A). This confound was reversed in a second condition, where the background was regularly alternating high and low pitched tones, and deviance was signaled by the repetition of a given pitch (Baudena, et al. 1995; Halgren, et al. 1995b; Halgren, et al. 1995c). In this case, deviant tones were more habituated than standards (see fig 1B). A comparison of the response to the two conditions suggested overlapping effects of habituation and deviance in the pSTP.

The same study found evidence for intracranial ERP generators to auditory stimulus deviance active before 200 ms in an attentional network that included the cingulate gyrus, subcallosal cortex, supramarginal gyrus, and dorsolateral prefrontal cortex (Baudena, et al. 1995; Halgren, et al. 1995b; Halgren, et al. 1995c). This activity was prolonged with locally generated P3a components that did not require overt attention in this simple auditory oddball paradigm. The earliest locally-generated P3a peaks occur in prefrontal cortex (Baudena, et al. 1995), where unilateral lesions can abolish the P3a over the entire scalp (Knight 1984), suggesting that the prefrontal cortex may perform essential antecedent calculations necessary for the P3a (Halgren 2008). At longer latencies, an even more extended network associated with the P3b generated activity to rare attended events, including hippocampus, ventromedial temporal cortex, the superior temporal sulcus, and a superior parietal region (Baudena, et al. 1995; Halgren, et al. 1995b; Halgren, et al. 1995c; Halgren, et al. 1980).

Since intracranial recording is the only method that can identify local generators with certainty, inferences from extracranial recordings need to be consistent with intracranial results (Halgren 2008). However, extracranial recordings can sample the entire brain whereas each intracranial contact only samples a small part of the brain. Furthermore, these data are obtained from patients with long standing epilepsy, especially in seizure-prone regions, and thus may be subject to contamination from the pathology. Finally, the intracranial studies have not included enough experimental contrasts to systematically explore the interactions of attention, dishabituation and deviance.

The current study uses magnetoencephalography to sequence the cortical activity evoked by rare shifts between two auditory tone sequences. A distributed inverse solution that constrained sources to lie on the cortical surface localized generators of successive ERP components in cortical areas consistent with previous intracranial recordings. We localize the earliest differential response to auditory pattern shifts to the STP even when the shifts are not confounded by sensory differences or dishabituation. Further, we demonstrate that the frontal lobe also generates a P3a in this task, but only to the attended rare target events. Overall, we find that the predominant neural activity evoked by rare target events appears to originate in superior temporal cortex during the MMN, involves frontal cortices during the N2 and P3a, and once again is centered in the anterior temporal lobe during the P3b.

## Methods

### Stimuli and Task

The later components of the electromagnetic fields reflecting cognitive processing of auditory stimuli are typically evoked and modulated using an `auditory oddball task.' In such tasks, rare tones of one pitch are randomly interspersed with frequent tones of another pitch. However, rarity is confounded with pitch, as well as sensory dishabituation (figure 1A). Nordby et al (1988) introduced a paradigm where tone pitch alternated on successive trials, with occasional rare repeated stimuli. In this case, the rare tones are more habituated, and their pitch is balanced with that of the frequent tones (figure 1B). In both cases, rarity and habituation are confounded. In the current study, we disentangled rarity from dishabituation by introducing a paradigm where the subject counted changes in the tone sequence between single-alternation (H-L-H-L-…) and double-alternation (HH-L-L-…) (figure 1C). Consequently, half of the rare events are indicated by tones that are a repeat of the preceding tone (e.g., H-L-H-L-**L**), and half are indicated by tones that are different (H-H-L-L-H-**L**). Pitch is balanced between rare and frequent tones. The same task was administered while the subject ignored the tones and read a book. Tones were 500 or 250Hz, 50 ms duration, with 500 ms from onset to onset. Task presentation was controlled by a MacIntosh computer (MacProbeTM software, Hunt 1994). The task was preceded by a practice period and after each block in the attend condition the subject was asked to indicate the number of shifts he had detected. Counts were always within 3 of the correct answer. In each block, 528 tones were presented, half high pitched and half low, including 47 rare tones (9% of the total). The number of frequent tones between successive rare tones was 7 to 13. The responses to the first 4 tones in each block, as well as to the first 2 tones after each rare tone, were omitted from analysis, in order to allow the brain response to stabilize. After these exclusions, there remained 84 habituated frequent and 299 dishabituated frequent tones. Two blocks were given with attention to stimuli, and two with ignoring stimuli (by reading a book). This task is designed to distinguish sensory dishabituation from pattern shift deviance, and their interaction with voluntary attention.

### Participants and Recording procedures

Eight healthy right-handed men (ages 20–26) served as volunteers. All were experienced in MEG experiments and selected on the basis of reliability and compliance with instructions. MEG signals were recorded from 306 channels at 0.1–200 Hz using a Neuromag-Vectorview instrument (Elekta, Stockholm) with a magnetometer and orthogonal pairs of planar gradiometers at each of 102 locations over the entire scalp. Unless otherwise noted, all analyses described below were performed on the 204 gradiometer channels only. Independent analyses were performed with magnetometer channels to confirm the gradiometer results. Head movement was minimized using an individually molded bitebar (Marinkovic, et al. 2004). Averages were low-pass filtered at 30 Hz prior to analysis. EEG referenced to the nose was recorded from standard midline sites Fz, Cz and Pz, using silver-

silver-chloride electrodes embedded in an electrode cap (Electro-Cap International, Inc.) with impedances less than 2 kΩ. The electrooculogram was recorded with bipolarly referred electrodes placed below the outer canthus of the right eye and just above the nasion with impedances less than 5 kΩ. Due to technical problems, only seven subjects provided EEG or magnetometer data of adequate quality to be analyzed; gradiometer data from all eight subjects were analyzed.

Prior to the MEG experiment, high-resolution 3-D T1-weighted magnetic resonance images (MRI) were acquired for each subject using a 1.5T Picker Eclipse (Marconi Medical, Cleveland, OH). The MEG sensor coordinate system was aligned with the MRI coordinate system using three head position (HPI) coils, attached to the scalp (Hamalainen, et al. 1993). The HPI coils generate weak magnetic signals, and thus can be directly localized by the MEG sensors. The positions of the HPI coils with respect to the subject's head (and thus MRI) were determined by measuring multiple points (including the HPI coils) using a Polhemus FastTrack 3-D digitizer. Trials from different conditions were averaged for each subject after rejecting trials with eyeblinks or other artifacts using amplitude criteria confirmed with visual inspection.

## Source Estimation

**Cortical surface reconstruction—**Geometrical representations of the cortical surface were constructed from the structural MRI using procedures described previously (Dale, et al. 1999; Dale and Sereno 1993; Fischl, et al. 1999a). First, the cortical white matter was segmented, and the estimated border between gray and white matter was tessellated, providing a topologically correct representation of the surface with ~150,000 vertices per hemisphere (Fischl, et al. 2001). For the inverse computation, the cortical surface was decimated to approximately 3000 dipoles per hemisphere (i.e., ~4mm spacing). Finally the folded surface tessellation was “inflated”, in order to unfold cortical sulci, thereby providing a convenient format for visualizing cortical activation patterns (Dale, et al. 1999; Dale and Sereno 1993; Fischl, et al. 1999a). For purposes of intersubject averaging, the reconstructed surface for each subject was morphed into an average spherical representation, optimally aligning sulcal and gyral features across subjects while minimizing metric distortions (Fischl, et al. 1999b).

**Forward solution—**The boundary element method (BEM) was used for calculating the signal expected at each MEG sensor, for each dipole location (deMunck 1992; Oostendorp and Van Oosterom 1992). The computation of the MEG forward solution has been shown to only require the inner skull boundary to achieve an accurate solution (Hamalainen and Sarvas 1989; Meijs, et al. 1987; Meijs and Peters 1987).

**Inverse solution—**To estimate the timecourses of cortical activity, the noise-normalized, anatomically-constrained linear estimation approach described in (Dale, et al. 2000) was used. This approach is similar to the generalized least-squares or weighted minimum norm solution (Dale and Sereno 1993; Hamalainen and Ilmoniemi 1984), but the estimate is normalized for noise sensitivity (Dale, et al. 2000). The noise-covariance was calculated from the 200 ms preceding the high minus low frequent tones (including both attend and ignored). The noise normalization has the effect of greatly reducing the variation in the point-spread function between locations (Liu, et al. 2002). This approach provides statistical parametric maps of cortical current dipoles, similar to the statistical maps typically generated using fMRI or PET data, but with a temporal resolution equal to the sampling rate.

A consequence of the dipole spacing used in the current study is that any given dipole would often need to represent a wide range of orientations. Thus, no *a priori* assumptions were

made about the local dipole orientation, and three components are required for each location. A sensitivity-normalized estimate of the local current dipole power (sum of squared dipole component strengths) at location *i* is given by

$$q_i(t) = \frac{\sum_{j \in G_i} \left( \mathbf{w}_j \cdot \mathbf{x}(t) \right)^2}{\sum_{j \in G_i} \mathbf{w}_j \mathbf{C} \mathbf{w}_j^T},$$

where $G_i$ is the set of (three) dipole component indices for the $i^{th}$ location, and $\mathbf{w}_i$ denotes the $i^{th}$ row of the inverse operator W (Dale, et al. 2000; Dale and Sereno 1993; Liu, et al. 1998). Note that under the null hypothesis, $q_i(t)$ is *F*-distributed, with three degrees of freedom for the numerator. The degrees of freedom for the denominator was 20 to 50, reflecting the number of time-samples used to calculate the noise covariance matrix C.

Inverse solutions were calculated in this manner every 5 ms for every condition and every individual. These movies were then averaged on the cortical surface across individuals after aligning their sulcal-gyral patterns. Conditions were compared by calculating the inverse solution from the subtraction sensor waveforms. The significance of activation at each site was then calculated using an F-test (Dale, et al. 2000; Dhond, et al. 2001), with a minimum significance threshold for all displayed activations chosen as $p<0.0001$. The significance of the comparisons between different conditions at particular conditions and latencies are directly indicated in the figures by these maps.

These significance levels give an indication of the reliability of the underlying activation. Furthermore, since the same noise covariance was used across conditions, the significance level at a given site can be used to compare its estimated activity across conditions. However, these localizations cannot be considered absolute, because the inverse problem is ill-posed unless strong *a priori* assumptions are applied that in the current context are certainly unjustified (Dale and Halgren 2001; Halgren 2008). Simulation studies indicate that by constraining the solution to lie on the individually reconstructed cortical surface and permitting distributed as well as focal solutions, that large errors are highly unlikely with the current technique (Dale, et al. 2000; Liu, et al. 1998). However, definitive localization of brain generators can only be obtained from detailed local field potential recordings (Halgren 2008). Such recordings have verified the gross accuracy of the current inverse methodology in localizing another distributed cognitive component, the N400m (Dale, et al. 2000). Furthermore, as discussed below, the current results are consistent with previous intracranial recordings using similar tasks in humans. Nonetheless, additional intracranial studies using an identical task are required to verify the localizations proposed in the current study.

**Sensor-level statistics—**In addition to the minimum norm source estimates described above, we conducted an independent analysis of our results using a random effects statistical approach, similar to that which is standard in many ERP studies. Paired t-tests were used to compare the average amplitude of selected sensors and latency ranges in each subject across conditions. Sensors were chosen that recorded in each subject from the frontal or temporal lobes, as determined from their cortical lead fields. Lead fields were calculated using forward solutions based on cortical and inner skull surfaces reconstructed from each individual's MRI. The contribution of each cortical dipole was normalized to that of the dipole contributing most strongly to the sensor in question. Since no inverse method was used in this analysis, and the forward solution is a well-posed biophysical calculation, these analyses allow the frontal and temporal contributions to the main findings to be examined without the ambiguities of inverse solutions.

# Results

## Overall pattern of response

Robust activity was recorded by sensors over both temporal and frontal lobes, especially to tones signaling rare attended pattern shifts (figure 3). Activity in all conditions began in the region of Heschl's gyrus before 100 ms, then involved more of the superior temporal lobe. Differential activity to rare stimuli initially involved postero-superior and polar temporal areas before 200 ms, spreading to cingulate and insular-opercular, then prefrontal (peaking from ~210–270 ms), and then back to temporal areas (peaking from ~340–450 ms), this time including ventral areas as well. This sequence was much attenuated, especially after ~270 ms, when the stimuli were ignored. Habituation decreased activity at ~160–240 ms in the superior temporal, opercular and posterior prefrontal regions.

## Scalp EEG

A limited sampling of scalp EEG was performed in order to confirm that the expected ERP components were evoked across the different task conditions. As expected, all tones evoked a negative-positive sequence corresponding to the previously described N1-P2 or N100-P200 (figure 2). These potentials were maximal at Cz where their latencies to peak for attended frequents were ~118 ms for N1, ~170 ms for P2a, and ~225 ms for P2b.

The effects of frequency-specific habituation and attention on the responses to frequent tones were studied (figure 2D–F). N1 was measured as a prominent negativity from 110–130 ms, and P2 as a P2a at 150–190 ms when it was maximal at Cz, and as P2b at 215–235 ms when it was maximal at Fz. Visual inspection suggested that habituation has little effect on N1 but diminishes P2a and P2b (figure 2D–E). Separate ANOVAs were performed for each component (N1, P2a, P2b) with factors of attention (attend, ignore), habituation (dishabituated, habituated), and site (Fz, Cz, Pz). No significant effects were found for N1. The main effects of habituation were significant for both P2a ($F(1,6)=19.576$, $p<.004$) and P2b ($F(1,6)=14.132$, $p<.009$). Attention had no significant effect on these components.

Although no MMN was obvious in the waveforms, we measured the average potential from 140–175 ms and tested for the effects of rarity and attention. Rarity and attention were not significant ($p>.3$), but a trend was observed for the three way interaction (attend × rarity × site: $F(1,6)=3.436$, $p<.066$). Later potentials, however, were strongly affected by rarity and/or attention. At Cz to rare attended tones, a sharp N2 peaking at ~225 ms is followed by a broad P3 with two peaks at ~290 ms and ~375 ms, labeled P3a and P3b, respectively (figure 2A). N2 is maximum frontally, P3a centrally, and P3b parietally. The N2 and P3a to rare tones appear to decrease when the tone sequence is ignored, and the P3b is abolished (compare figure 2A vs 2B). N2, P3a, and P3b were measured as average amplitudes from 215–235 ms, 280–300 ms, and 365–385 ms, respectively, relative to a 100 ms pre-stimulus baseline (figure 2C). Separate ANOVAs with factors of attention (attend, ignore), rarity (rare, frequent), and site (Fz, Cz, Pz) were performed for each component (N2b, P3a, P3b). For N2, the main effect of rarity was significant ($F(1,6)=8.001$, $p<.030$). For P3a, the main effects of rarity ($F(1,6)=15.456$, $p<.008$) and site ($F(2,12)=5.268$, $p<.023$) were significant as was the interaction of rarity × site ($F(2,12)=12.960$, $p<.001$). For P3b, the main effects of attention ($F(1,6)=8.986$, $p<.024$), rarity ($F(1,6)=11.602$, $p<.014$) and site ($F(2,12)=38.989$, $p<.001$) were significant, as were interactions of rarity × site ($F(2,12)=33.947$, $p<.001$), attention × site ($F(2,12)=69.420$, $p<.001$), and attention × rarity × site ($F(2,12)=27.516$, $p<.001$). Thus, rare shifts in tone patterns evoke a negativity at ~225 ms followed by a bi-peaked positivity that is strongly modulated by attention.

### Early activity in all conditions

Initial activity was localized to the posterior superior temporal plane (sTp) and adjacent structures including the superior temporal sulcus (sTs), from ~55 to ~155 ms, more prominent on the right. This pattern was observed to attended and ignored, rare and frequent, dishabituated and habituated stimuli. It is illustrated at latencies of 100 and 130 ms in figure 4.

### Rare versus frequent tones

Following these early responses, attended rare stimuli evoke mainly fronto-temporal activity from ~180 ms to the next tone onset at 500 ms. Two peaks of this activity, at 230 and 370 ms are shown in Figure 4. The earlier peak was centered in the posteroventral frontal cortex (pvF), with additional activity in the insulo-opercular (IO), dorsolateral prefrontal (dlpF), and orbitofrontal (oF) cortices, as well as continuing activity in temporal lobe structures including the temporal pole (Tp), sTs and sTp. At the longer latency, little frontal activity remained, and the temporal activity had spread posteriorly to reach the temporo-parieto-occipital junction (TPO). Especially at 370 ms, activity was more prominent in the right hemisphere.

In order to better appreciate the spatiotemporal evolution of activity specific to attended rare stimuli, the activity evoked by frequent tones was subtracted and the generators of the difference waveforms were estimated. Snapshots of this activity made every 10 ms from 130 to 420 ms after the stimulus are shown in figure 5. Peaks of activity were observed at ~230 and 370 ms. Note that the patterns of activity observed at these peaks are similar to those observed at the same latencies to unsubtracted rare tones (in figure 4), because frequent tones evoke little activity after ~180 ms.

Following the earliest differential activity in the Tp at ~130 ms, there was a progressive involvement of insulo-opercular and more posterior temporal areas, first the sTp, then sTs extending to TPO by ~190 ms. After this point, differential activity becomes increasingly frontal, especially pvF but also dlpF and oF, and still including the IO and temporal areas. While this frontally-dominant pattern peaked at ~230 ms, it was still visible until ~300 ms, at which time activity started to shift again toward the temporal lobe. This pattern increased in strength until ~350 ms and then remained at a high level throughout the recording epoch (until 500 ms). At longer latencies (>~380 ms), TPO involvement was increasingly prominent.

The finding that the earliest differential activity to rare attended tones in the right hemisphere localized to Tp was also obtained in the left hemisphere, as is shown in a ventral view in figure 6a. The initial right Tp onset was also found to attended rare tones when activity was localized using magnetometer rather than gradiometer measurements (figure 6c), as well as to ignored rare tones (figure 6d).

Prominent differential activity to rare tones was also observed on the medial cortex, beginning in the anterior cingulate region (aC) below the genu of the corpus callosum at ~150 ms (figure 7). Activity spread to middle cingulate (mC) and posterior cingulate (pC) regions by ~230 ms, but was more sustained in aC at 260 ms, declining at longer latencies. Thus, aC activity generally followed the same time-course as was observed for lateral frontal activity. At the longer latencies, when lateral activity WAs centered on the temporal lobe, medial activity also shifted to medial temporal (mT) and Tp sites (see, for example, at 370 ms in figure 7).

### Magnetometers versus Gradiometers

Analyses with the 102 axial magnetometer channels substantially confirmed those obtained with the 204 planar gradiometer channels. This is illustrated in figure 8 for snapshots at 5 latencies of estimated source configurations evoked by attended rare minus frequent stimuli. The same comparison is shown for an earlier latency in figure 6. Activity estimated from either magnetometers or gradiometers began at ~130 ms in the region of Tp, spread to involve much of the temporal lobe (including sTp, sTs and TPO) by 195 ms, then shifted frontally (centered in pvF, including also oF, dlpF) to peak at ~230 ms, then back to temporal sites reaching high levels by ~370 ms and continuing to the end of the recording.

Although the overall patterns were identical, small differences could be noted. The most salient was a greater tendency for activity estimated from magnetometers to be present in ventral occipitotemporal (vOT) and TPO regions. In the Rolandic region, activity estimated from gradiometers had a greater tendency to be located in the subcentral gyrus whereas that from magnetometers tended to be located in the more dorsal precentral gyrus. These relatively minor differences would not materially affect the conclusions of this study; rather, the magnetometer data indicate that analyses based on different sets of sensors with quite different lead fields and noise characteristics yielded similar time-courses and locations of activity.

### Dishabituated versus habituated tones

Sources were estimated for differential activity evoked by late frequent tones that were preceded by a tone of the same pitch (`habituated') versus those that were preceded by a tone of the opposite pitch (`dishabituated'). The resulting spatiotemporal patterns for the attend and ignore conditions are shown in figure 9. The earliest differential activity to attended dishabituated tones was estimated to the posterior sTp at ~80 ms. This activity increased and spread to sTs and pvF by ~165 ms, peaking in the same areas at ~195 ms, was over by ~250 ms. Compared to attended dishabituated tones, ignored dishabituated tones evoked differential activity with similar strength, duration and anatomical distribution. The spatiotemporal pattern to ignored dishabituated tones was delayed by ~45 ms, with a peak at ~230 ms. Thus, in contrast to the multiple spatial patterns evoked at different latencies by rare target tones, differential activity to dishabituated tones exhibited a single spatial pattern with a single peak.

### Attended versus Ignored tones

Figure 9 also shows the effects of attention on the differential activity evoked by rare as compared to frequent tones. The differential effects of rare pattern shifts were largely abolished when the tones were ignored. The little activity which did remain peaked at ~230 ms and had a similar (but much weaker) distribution to that observed at the same latency to attended stimuli, involving frontotemporal locations, primarily pvF, IO, sTp and sTs. This spatial pattern of differential activity evoked by ignored rare stimuli at ~230 ms was similar to but smaller than the differential activity evoked by ignored dishabituated stimuli at the same latency. This powerful enhancement of rarity effects by attention stands in contrast with the lack of pronounced effects of attention on the size of dishabituation effects.

### Sensor-level MEG comparisons

The main results described above were confirmed using a random effects statistical approach that is standard in many ERP studies. Specifically, we selected one sensor over the frontal lobe, and measured the average amplitude in each subject of the MEG signal in a 20 ms window centered on 230 ms (figure 3). These measurements were found to be significantly different ($p<.02$) when compared between attended rare and late frequent tones

using two-tailed paired t-tests. A similar analysis was conducted for measurements by one sensor over the temporal lobe centered on 370 ms, and again was found to be significantly different ($p<.002$). The cortical lead fields of the frontal and temporal sensors used in each subject for this analysis were shown to be limited to the respective frontal and temporal lobes (please see Methods, and figure 10). Thus, using an approach that is not limited by the uncertainties which are inherent in all inverse estimates, we confirmed that selective responses to rare events are generated at ~230ms after stimulus onset in the frontal lobe, and at ~370ms in the temporal lobe.

## Discussion

Rare unpredictable shifts in the pattern of an ongoing tonal sequence evoked MEG responses that were mainly localized to first temporal, then frontal, and then again temporal areas. Following the earliest differential activity in the temporal pole shortly after 100 ms, there is a progressive involvement of insulo-opercular and more posterior temporal areas, first the superior temporal plane, and then the superior temporal sulcus extending to the temporo-parieto-occipital junction before 200 ms. In the scalp EEG, deviant stimuli evoke in this latency range an attention-sensitive mismatch negativity (aMMN). Cognitively, this stage may reflect the initial detection of the change in the tonal sequence. After 200 ms, differential activity becomes increasingly frontal, especially in posteroventral prefrontal cortex, but extending to dorsolateral, orbital and medial areas. This frontally-dominant pattern peaks at ~230 ms when it corresponds to N2 at the scalp, and may reflect updating of an internal rhythmic template. The frontal pattern extends to about 300 ms, at which time it overlaps with the scalp P3a component. Activity then shifts back to the temporal lobe, where it increases in strength until ~350 ms and remains at a high level until the end of the recording epoch at 500 ms. This processing phase corresponds to the scalp P3b and may underlie definitive identification of the event and cognitive closure. All phases are strongly lateralized to the right hemisphere. These results have implications for the spatiotemporal organization of the cortical events underlying musical processing, as well as the localization of the generators of common endogenous potentials **in all modalities**.

### Early temporal lobe generation of activity during the aMMN

In the current task, half of the tones signaling a pattern shift matched the preceding tone in pitch, and half did not. Previous studies of scalp ERPs have shown that the effects of frequency-specific habituation depend only on the first prior interval (Roth, et al. 1976). Thus, unlike most prior studies of the MMN, N2 and P3, in the current study sensory dishabituation was dissociated from rarity. Furthermore, our results show that dishabituation itself evokes a similar distribution of activity, localized to the superior temporal and posterior prefrontal cortices, as that evoked by rare pattern shifts. The dishabituation effects are very small compared to rarity in the attend condition, but are larger than the rarity effect during the ignore condition. Thus, it is important to control for dishabituation when one is attempting to identify responses to ignored rare stimuli.

Classically, the mismatch negativity (MMN) results from a preattentive mismatch detection process that initiates involuntary switching of attention to an auditory stimulus change outside the focus of attention (Naatanen 1992). Previous studies have found that a `deviance related negativity' can be evoked by shifts in the global pattern of the prior several tones, as well as the local shift from the immediately preceding tone (Horvath, et al. 2001). This negativity has been interpreted as a MMN, based on its scalp topography and its latency of 125–210 ms (Alain, et al. 1999; Horvath, et al. 2001; Nordby, et al. 1988). Although this pattern-shift MMN occurs even when the tone sequence is ignored, it is strongly modulated by attention (Alain and Woods 1997; Horvath, et al. 2001). In a similar but somewhat more complex paradigm, rare melodic events evoked both the MMN and P3 when attended but

only the MMN when ignored (Trainor, et al. 2002). The current study shows that these characteristics also obtain for the pattern-shift MMNm as recorded with MEG- it does not require attention but is strongly modulated by it, has an onset latency of about 125 ms, and it is associated with later components only if the tone pattern is attended.

In the current study, most differential activity prior to 200 ms was localized to the superior temporal region. Our findings confirm superior temporal generation of the MMN at early latencies in a global pattern shift paradigm. However, an unexpected finding was that the earliest differential activity to rare events, at latencies of 95–130 ms, localized to the anterior temporal lobe. This was noted in the left and right hemispheres, in the ignore and attend conditions, and with gradiometers as well as magnetometers. MMN-like potentials have previously been recorded from medioventral and polar temporal cortices but not until about 200 ms after stimulus onset (Halgren, et al. 1995d; Rosburg, et al. 2007). Furthermore, hippocampal lesions did not affect the MMN (Alain, et al. 1998; Alho, et al. 1994). On the other hand, hippocampal formation lesions do influence the related P3a to novel stimuli (Knight 1996). Furthermore, the hippocampal formation receives direct input from auditory association cortex (Blatt, et al. 2003), and rare units in the posterior hippocampus respond to simple auditory stimuli with a latency of ~100 ms, and show strong habituation (Wilson, et al. 1984). Thus, it remains possible that the anteroventromedial temporal region works with the superior temporal cortex in detecting mismatches, but further confirmation with intracranial recordings is necessary.

### Frontal generators during the N2 and P3a

Our MEG results suggest that between ~210 and 290 ms, differential activation to attended rare events is mainly localized to the frontal lobe, especially the right posteroventral frontal and anterior cingulate areas. Activity localized to the temporal lobe continues during this period but is weaker than frontal activity, and is also weaker than earlier and later temporal activity. Differential activation to ignored rare events was much weaker but was localized to similar areas.

During this latency range, intracranial recordings have found that the P3a occurs as part of a triphasic waveform with peaks at 210, 280 and 390 ms in several frontal sites, regardless of attention (Alain, et al. 1989; Baudena, et al. 1995; Smith, et al. 1990). The largest amplitudes were near the inferior frontal sulcus, with clear polarity inversions in the anterior cingulate and subgenual cortices (Baudena, et al. 1995). Novel stimuli may evoke BOLD activation in similar areas (Bledowski, et al. 2004; Clark, et al. 2000; Downar, et al. 2001; Kiehl, et al. 2001; Linden, et al. 1999; McCarthy, et al. 1997). In the current study, the shift seen at the scalp EEG, between a fronto-centrally maximum N2 and P3a peaking at ~220 and ~290 ms, to a parietally maximum P3b peaking at ~375 ms, corresponded well to the shift in the predominant locus of MEG activation from fronto-cingulate at 210–290 ms to temporal at 375 ms. Thus, the current findings are highly consistent with prior intracranial recordings in humans, except that in the current study, the scalp P3a was greatly attenuated when the stream was ignored, presumably because attention was required in order to detect the shift from single to double alternation.

### Late temporal lobe processing and generation of the P3b

Predominant generation of the P3b in the temporal lobe also corresponds well to previous intracranial recordings. The largest and most consistent cerebral generator active during the P3b is in the hippocampus. Evidence for local generation includes: (1) large amplitude (Brazdil, et al. 1999; Brazdil, et al. 2003; Clarke, et al. 1999; Grunwald, et al. 1999; Halgren, et al. 1995c; Halgren, et al. 1980; Kanovsky, et al. 2003; McCarthy, et al. 1989; Puce, et al. 1989; Smith, et al. 1990; Squires, et al. 1983; Stapleton and Halgren 1987;

Watanabe, et al. 2002); (2) steep voltage gradients (Halgren, et al. 1995c; McCarthy, et al. 1989); (3) correlated unit activity (Halgren, et al. 1983); and (4) local amplitude decrements associated with local lesions (Grunwald, et al. 1999; Puce, et al. 1989; Squires, et al. 1983). However, hippocampal lesions (Onofrj, et al. 1992; Polich and Squire 1993) have little or no influence on the scalp P3 potential, and with rare exceptions (Kiehl, et al. 2001), BOLD recordings also fail to detect the hippocampal response (Halgren 2008). MEG may be more successful, with medial temporal P3b sources estimated to auditory (Nishitani, et al. 1998; Tarkka, et al. 1995) and visual stimuli (Basile, et al. 1997; Okada, et al. 1983). Confirmation of local generation was obtained when this source was lost ipsilaterally after unilateral anterior temporal lobectomy (Nishitani, et al. 1999). However, it is also possible that the MEG signal is actually arising in medioventral temporal structures outside the hippocampus (Halgren, et al. 1995c; Halgren, et al. 1980; Stapleton and Halgren 1987).

In addition to the medial temporal lobe, previous MEG studies have found P3b sources in the inferior parietal lobule (Nishitani, et al. 1998) and superior temporal sulcus (Basile, et al. 1997). Cortical Potential Imaging of high-density EEG estimated P3b sources mainly to the left superior parietal lobule and posteromedial frontal cortex (He, et al. 2001). Interestingly, the ventral temporal and ventral prefrontal sources demonstrated with intracranial recordings were not detected. These observations are consistent with the large P3b decrements in typical auditory oddball tasks that are found after temporo-parietal lesions (Knight 1990; Soltani and Knight 2000). The inferior parietal and lateral temporal generators inferred from MEG may reflect the generators inferred from the large amplitude steeply changing intracranial P3b's recorded in a limited region of the superior temporal sulcus, and, more rarely, in the parietal lobe (Halgren, et al. 1995b; Halgren, et al. 1995c; Smith, et al. 1990). These regions are also the most commonly activated by rare target events in BOLD recordings (for review see (Linden 2005)). The current study is consistent with these results, with activity during the P3b localized to the superior temporal sulcus, which extends posteriorly to the temporoparieto-occipital junction. However, in the parietal lobe, the MEG and intracranial P3b localizations are generally ventral to those inferred from BOLD.

Additional sources of the auditory P3b were localized using MEG to the superior temporal plane (Nishitani, et al. 1998; Tarkka, et al. 1995). This may reflect the modality-specific activity to rare auditory events that has been recorded intracranially in the superior temporal plane (Halgren, et al. 1995a). This activity occurred to ignored stimuli in a simple oddball task, and it was not dissociated from dishabituation. The strong activity during the P3b localized to the superior temporal plane in the current study demonstrate that this activity is independent of dishabituation, and suggests that it can be dependent on overt attention if identification of the rare event is relatively difficult.

Some previous MEG studies have estimated P3b generators to the thalamus rather than the medial temporal lobe (Mecklinger, et al. 1998; Rogers, et al. 1991). A similar localization was reported for the P3b-like activity identified using Independent Component Analysis applied to high-density EEG (Makeig, et al. 2004). These studies failed to identify the parietal, temporal and prefrontal generators demonstrated with intracranial recordings. Numerous intracranial studies have reported thalamic potentials with the latency and task correlates of the P3 (Katayama, et al. 1985; Klostermann, et al. 2006; Kropotov and Ponomarev 1991; Rektor, et al. 2001; Velasco, et al. 1989; Yingling and Hosobuchi 1984). In published examples, these potentials are often small and do not exhibit steep complex gradients or inversions. Such potentials could reflect passive volume conduction from the cortex rather than local generation (Klee and Rall 1977). Indeed, pyramidal cells arrayed in cortical palisades are far better suited to generate the aligned currents that generate MEG (Halgren 2008), and even if generated, such fields will propagate very weakly to extracranial

sensors (Cohen and Cuffin 1983). For these reasons, our method does not seek to estimate activity in thalamic dipoles (Dale, et al. 2000).

### The cerebral processing stream for tone sequences

In summary, the current results found three phases. The initial superior temporal lobe activity occurs during the MMN and thus presumably reflects detection of the shift in the tonal sequence (Naatanen 1992). The second phase is localized to the frontal lobe, occurs during the N2 and P3a, and thus may reflect the orientation of attention (Marinkovic, et al. 2001). The third phase is again temporal, and occurs during the P3b, which has been associated with cognitive closure and updating of working memory (Donchin, et al. 1983; Verleger 2008). A potential caveat to the current results is that the task is more difficult and has different temporal dynamics than the typical auditory oddball task. Thus, it would be important to confirm the localization of these components using other tasks and sensory modalities.

In addition to functioning as a well-controlled means for evoking classical endogenous potential components (MMN, N2, P3a and P3b), the current task probes a fundamental aspect of music, detecting shifts in tonal sequences. Neuropsychological studies have shown that the right superior temporal plane anterior to Heschl's gyrus is important for the discrimination of tonal contours or melodies (Liegeois-Chauvel, et al. 1998). Direct recordings from auditory cortex suggests a specialization of the right hemisphere for pitch discrimination (Liegeois-Chauvel, et al. 2001). Tonal working memory is also impaired by right prefrontal lesions (Zatorre 2001). PET and fMRI studies implicate the right superior temporal gyrus in detecting the relations between pitches, interacting with prefrontal cortex where tonal sequences are stored in working memory (Zatorre, et al. 1994). In the crucial comparison, increased working memory load for comparing the pitch of two tones resulted in increased blood flow in the right ventrolateral prefrontal cortex, with secondary foci in the homologous left site, and in the anterior cingulate (Zatorre 2001). In monkeys, ventrolateral prefrontal neurons are reciprocally connected with the anterior superior temporal plane and fire to complex sounds (Romanski and Goldman-Rakic 2002; Romanski, et al. 1999).

These locations are strikingly similar to those observed in our study with MEG. The current results add to these previous findings in allowing their temporal dynamics to be appreciated, and related to generic cognitive processes indexed by well-studied endogenous ERP components. These reveal an initial stage of high-level mismatch detection from ~140–190 ms, relying on the superior temporal plane, possibly interacting with anteromedial temporal cortex. From ~210–290 ms, prefrontal and cingulate activity dominates, perhaps probing working memory and engaging attention. Finally, from ~340–500 ms, the temporal lobe is again reactivated, now including its ventromedial as well as superior aspects, associated with definitive identification of the pattern change, and updating of working memory as part of cognitive closure. The updated template sent from the prefrontal working memory and predictive circuits to the temporal lobe would permit the later to detect the next change.

## Acknowledgments

Supported by USPHS (NIH grants NS18741 and AA016624). We thank Nathalie Christensen, Valerie Carr, Jeffrey Lewine, Kim Paulson, Bruce Fischl, and Thomas Witzel.

## References

Alain C, Achim A, Woods DL. Separate memory-related processing for auditory frequency and patterns. Psychophysiology. 1999; 36(6):737–44. [PubMed: 10554587]

Alain C, Richer F, Achim A, Saint-Hilaire JM. Human intracerebral potentials associated with target, novel and omitted auditory stimuli. Brain Topography. 1989; 1:237–245. [PubMed: 2641266]

Alain C, Woods DL. Attention modulates auditory pattern memory as indexed by event-related brain potentials. Psychophysiology. 1997; 34(5):534–46. [PubMed: 9299908]

Alain C, Woods DL, Knight RT. A distributed cortical network for auditory sensory memory in humans. Brain Res. 1998; 812(1–2):23–37. [PubMed: 9813226]

Alho K, Woods DL, Algazi A, Knight RT, Näätänen R. Lesions of frontal cortex diminish the auditory mismatch negativity. Electroencephalography and Clinical Neurophysiology. 1994; 91(5):353–62. [PubMed: 7525232]

Basile LF, Rogers RL, Simos PG, Papanicolaou AC. Magnetoencephalographic evidence for common sources of long latency fields to rare target and rare novel visual stimuli. Int J Psychophysiol. 1997; 25(2):123–37. [PubMed: 9101337]

Baudena P, Heit G, Clarke JM, Halgren E. Intracerebral potentials to rare target and distractor auditory and visual stimuli: 3. Frontal cortex. Electroencephalography and Clinical Neurophysiology. 1995; 94:251–264. [PubMed: 7537197]

Blatt GJ, Pandya DN, Rosene DL. Parcellation of cortical afferents to three distinct sectors in the parahippocampal gyrus of the rhesus monkey: an anatomical and neurophysiological study. J Comp Neurol. 2003; 466(2):161–79. [PubMed: 14528446]

Bledowski C, Prvulovic D, Hoechstetter K, Scherg M, Wibral M, Goebel R, Linden DE. Localizing P300 generators in visual target and distractor processing: a combined event-related potential and functional magnetic resonance imaging study. J Neurosci. 2004; 24(42):9353–60. [PubMed: 15496671]

Brazdil M, Rektor I, Dufek M, Daniel P, Jurak P, Kuba R. The role of frontal and temporal lobes in visual discrimination task-- depth ERP studies. Neurophysiol Clin. 1999; 29(4):339–50. [PubMed: 10546252]

Brazdil M, Roman R, Daniel P, Rektor I. Intracerebral somatosensory event-related potentials: effect of response type (button pressing versus mental counting) on P3-like potentials within the human brain. Clin Neurophysiol. 2003; 114(8):1489–96. [PubMed: 12888032]

Clark VP, Fannon S, Lai S, Benson R, Bauer L. Responses to rare visual target and distractor stimuli using event- related fMRI. J Neurophysiol. 2000; 83(5):3133–9. [PubMed: 10805707]

Clarke JM, Halgren E, Chauvel P. Intracranial ERP recordings during a lateralized visual oddball task: 2. temporal, parietal and frontal recordings. Electroencephalography and Clinical Neurophysiology. 1999; 110:1226–1244.

Cohen D, Cuffin BN. Demonstration of useful differences between magnetoencephalogram and electroencephalogram. Electroencephalography and Clinical Neurophysiology. 1983; 56:38–51. [PubMed: 6190632]

Csepe V, Karmos G, Molnar M. Evoked potential correlates of stimulus deviance during wakefulness and sleep in cat--animal model of mismatch negativity. Electroencephalogr Clin Neurophysiol. 1987; 66(6):571–8. [PubMed: 2438122]

Dale AM, Fischl B, Sereno MI. Cortical surface-based analysis I: Segmentation and surface reconstruction. NeuroImage. 1999; 9(2):179–94. [PubMed: 9931268]

Dale AM, Halgren E. Spatiotemporal mapping of brain activity by integration of multiple imaging modalities. Current Opinion in Neurobiology. 2001; 11:202–8. [PubMed: 11301240]

Dale AM, Liu AK, Fischl BR, Buckner RL, Belliveau JW, Lewine JD, Halgren E. Dynamic statistical parametric mapping: combining fMRI and MEG for high-resolution imaging of cortical activity. Neuron. 2000; 26(1):55–67. [PubMed: 10798392]

Dale AM, Sereno MI. Improved localization of cortical activity by combining EEG and MEG with MRI cortical surface reconstruction: A linear approach. Journal of Cognitive Neuroscience. 1993; 5:162–176.

deMunck JC. A linear dicretization of the volume conductor boundary integral equation using analytically integrated elements. IEEE Transactions on Biomedical Engineering. 1992; 39:986–990. [PubMed: 1473829]

Dhond RP, Buckner RL, Dale AM, Marinkovic K, Halgren E. Spatiotemporal maps of brain activity underlying word generation and their modification during repetition priming. J Neurosci. 2001; 21(10):3564–71. [PubMed: 11331385]

Donchin, E.; McCarthy, G.; Kutas, M.; Ritter, W. Event-related potentials in the study of consciousness. In: Davidson, RJ.; Schwartz, GE.; Shapiro, D., editors. Consciousness and Self-Regulation. Advances in Research and Theory. Vol. Vol. 3. Plenum; New York: 1983. p. 81-122.

Downar J, Crawley AP, Mikulis DJ, Davis KD. The effect of task relevance on the cortical response to changes in visual and auditory stimuli: an event-related fMRI study. Neuroimage. 2001; 14(6): 1256–67. [PubMed: 11707082]

Fischl B, Liu A, Dale AM. Automated manifold surgery: constructing geometrically accurate and topologically correct models of the human cerebral cortex. IEEE Trans Med Imaging. 2001; 20(1): 70–80. [PubMed: 11293693]

Fischl B, Sereno MI, Dale AM. Cortical surface-based analysis II: Inflation, flattening, a surface-based coordinate system. NeuroImage. 1999a; 9(2):195–207. [PubMed: 9931269]

Fischl B, Sereno MI, Tootell RB, Dale AM. High-resolution intersubject averaging and a coordinate system for the cortical surface. Hum Brain Mapp. 1999b; 8(4):272–84. [PubMed: 10619420]

Giard MH, Perrin F, Pernier J, Bouchet P. Brain generators implicated in the processing of auditory stimulus deviance: A topographic event-related potential study. Psychophysiology. 1990; 27:627–640. [PubMed: 2100348]

Grunwald T, Beck H, Lehnertz K, Blumcke I, Pezer N, Kutas M, Kurthen M, Karakas HM, Van Roost D, Wiestler OD, et al. Limbic P300s in temporal lobe epilepsy with and without Ammon's horn sclerosis. Eur J Neurosci. 1999; 11(6):1899–906. [PubMed: 10336658]

Halgren, E. Considerations in source estimation of the P3. In: Ikeda, A.; Inoue, Y., editors. Event-related Potentials in Patients with Epilepsy. John Libbey Eurotext; Paris: 2008.

Halgren E, Baudena P, Clarke JM, Heit G, Liégeois-Chauvel C, Chauvel P, Musolino A. Intracerebral potentials to rare target and distractor auditory and visual stimuli: 1. Superior temporal plane and parietal lobe. Electroencephalography and Clinical Neurophysiology. 1995a; 94:191–220. [PubMed: 7536154]

Halgren E, Baudena P, Clarke JM, Heit G, Liégeois C, Chauvel P, Musolino A. Intracerebral potentials to rare target and distractor auditory and visual stimuli. I. Superior temporal plane and parietal lobe. Electroencephalography and Clinical Neurophysiology. 1995b; 94(3):191–220. [PubMed: 7536154]

Halgren E, Baudena P, Clarke JM, Heit G, Marinkovic K, Devaux B, Vignal JP, Biraben A. Intracerebral potentials to rare target and distractor auditory and visual stimuli. II. Medial, lateral and posterior temporal lobe. Electroencephalography and Clinical Neurophysiology. 1995c; 94(4): 229–50. [PubMed: 7537196]

Halgren E, Baudena P, Clarke JM, Heit G, Marinkovic K, Devaux B, Vignal JP, Biraben A. Intracerebral potentials to rare target and distractor auditory and visual stimuli: 2. Medial, lateral and posterior temporal lobe. Electroencephalography and Clinical Neurophysiology. 1995d; 94(4): 229–250. [PubMed: 7537196]

Halgren E, Squires NK, Wilson CL, Rohrbaugh JW, Babb TL. Endogenous potentials generated in the human hippocampal formation and amygdala by infrequent events. Science. 1980; 210:803–805. [PubMed: 7434000]

Halgren, E.; Wilson, CL.; Squires, NK.; Engel, J.; Walter, RD.; Crandall, PH. Dynamics of the human hippocampal contribution to memory. In: Seifert, W., editor. Neurobiology of the Hippocampus. Academic; London: 1983. p. 529-572.

Hamalainen M, Hari R, Ilmoniemi RJ, Knuutila J, Lounasmaa OV. Magnetoencephalography - theory, instrumentation, and application to noninvasive studies of the working human brain. Reviews of Modern Physics. 1993; 65:413–497.

Hamalainen, MS.; Ilmoniemi, RJ. Interpreting measured magnetic fields of the brain: estimates of current distributions. Helsinki Univ. of Technology; Helsinki, Finland: 1984.

Hamalainen MS, Sarvas J. Realistic conductivity geometry model of the human head for interpretation of neuromagnetic data. IEEE Trans. Biomed. Eng. 1989; 36:165–171. [PubMed: 2917762]

Hari R, Hamalainen M, Ilmoniemi R, Kaukoranta E, Reinikainen K, Salminen J, Alho K, Naatanen R, Sams M. Responses of the primary auditory cortex to pitch changes in a sequence of tone pips: neuromagnetic recordings in man. Neurosci Lett. 1984; 50(1–3):127–32. [PubMed: 6493619]

He B, Lian J, Spencer KM, Dien J, Donchin E. A cortical potential imaging analysis of the P300 and novelty P3 components. Hum Brain Mapp. 2001; 12(2):120–30. [PubMed: 11169876]

Horvath J, Czigler I, Sussman E, Winkler I. Simultaneously active pre-attentive representations of local and global rules for sound sequences in the human brain. Brain Res Cogn Brain Res. 2001; 12(1):131–44. [PubMed: 11489616]

Hunt SMJ. MacProbe: A Macintosh-based experimenter's workstation for the cognitive sciences. Behavioral Research Methods,Instrumentation and Computing. 1994; 26:345–351.

Jaaskelainen IP, Ahveninen J, Bonmassar G, Dale AM, Ilmoniemi RJ, Levanen S, Lin FH, May P, Melcher J, Stufflebeam S, et al. Human posterior auditory cortex gates novel sounds to consciousness. Proc Natl Acad Sci U S A. 2004; 101(17):6809–14. [PubMed: 15096618]

Javitt DC, Steinschneider M, Schroeder CE, Vaughan HG Jr. Arezzo JC. Detection of stimulus deviance within primate primary auditory cortex: intracortical mechanisms of mismatch negativity (MMN) generation. Brain Res. 1994; 667(2):192–200. [PubMed: 7697356]

Kanovsky P, Streitova H, Klajblova H, Bares M, Daniel P, Rektor I. The impact of motor activity on intracerebral ERPs: P3 latency variability in modified auditory odd-ball paradigms involving a motor task. Neurophysiol Clin. 2003; 33(4):159–68. [PubMed: 14519543]

Katayama Y, Tsukiyama T, Tsubokawa T. Thalamic negativity associated with the endogenous late positive component of cerebral evoked potentials (P300): Recordings using discriminative aversive conditioning in humans and cats. Brain Research Bulletin. 1985; 14:223–226. [PubMed: 3995364]

Kiehl KA, Laurens KR, Duty TL, Forster BB, Liddle PF. Neural sources involved in auditory target detection and novelty processing: an event-related fMRI study. Psychophysiology. 2001; 38(1): 133–42. [PubMed: 11321614]

Klee M, Rall W. Computed potentials of cortically arranged populations of neurons. Journal of Neurophysiology. 1977; 40:647–666. [PubMed: 874533]

Klostermann F, Wahl M, Marzinzik F, Schneider GH, Kupsch A, Curio G. Mental chronometry of target detection: human thalamus leads cortex. Brain. 2006; 129(Pt 4):923–31. [PubMed: 16418179]

Knight, R. Neural mechanisms of event-related potentials: Evidence from human lesion studies. In: Rohrbaugh, JW.; Parasuraman, R.; Johnson, R., editors. Event-related brain potentials: basic issues and applications. Oxford University Press; New York: 1990. p. 3-18.

Knight R. Contribution of human hippocampal region to novelty detection. Nature. 1996; 383(6597): 256–9. [PubMed: 8805701]

Knight RT. Decreased response to novel stimuli after prefrontal lesions in man. Electroencephalography and Clinical Neurophysiology. 1984; 59:9–20. [PubMed: 6198170]

Knight RT, Scabini D, Woods DL, Clayworth CC. The effects of lesions of superior temporal gyrus and inferior parietal lobe on temporal and vertex components of the human AEP. Electroencephalography and Clinical Neurophysiology. 1988; 70:499–509. [PubMed: 2461284]

Kropotov JD, Alho K, Naatanen R, Ponomarev VA, Kropotova OV, Anichkov AD, Nechaev VB. Human auditory-cortex mechanisms of preattentive sound discrimination. Neurosci Lett. 2000; 280(2):87–90. [PubMed: 10686384]

Kropotov JD, Näätänen R, Sevostianov AV, Alho K, Reinikainen K, Kropotova OV. Mismatch negativity to auditory stimulus change recorded directly from the human temporal cortex. Psychophysiology. 1995; 32:418–422. [PubMed: 7652119]

Kropotov JD, Ponomarev VA. Subcortical neuronal correlates of component P300 in man. Electroencephalography and Clinical Neurophysiology. 1991; 78(1):40–9. [PubMed: 1701714]

Liegeois-Chauvel C, Giraud K, Badier JM, Marquis P, Chauvel P. Intracerebral evoked potentials in pitch perception reveal a functional asymmetry of the human auditory cortex. Ann N Y Acad Sci. 2001; 930:117–32. [PubMed: 11458823]

Liegeois-Chauvel C, Peretz I, Babai M, Laguitton V, Chauvel P. Contribution of different cortical areas in the temporal lobes to music processing. Brain. 1998; 121(Pt 10):1853–67. [PubMed: 9798742]

Linden DE, Prvulovic D, Formisano E, Vollinger M, Zanella FE, Goebel R, Dierks T. The functional neuroanatomy of target detection: an fMRI study of visual and auditory oddball tasks. Cereb Cortex. 1999; 9(8):815–23. [PubMed: 10601000]

Linden DEJ. The P300: Where in the brain is it produced and what does it tell us? The Neuroscientist. 2005; 11:563–576. [PubMed: 16282597]

Liu AK, Belliveau JW, Dale AM. Spatiotemporal imaging of human brain activity using fMRI constrained MEG data: Monte Carlo simulations. Proceedings of the National Academy of Sciences of the United States of America. 1998; 95:8945–8950. [PubMed: 9671784]

Liu AK, Dale AM, Belliveau JW. Monte Carlo simulation studies of EEG and MEG localization accuracy. Hum Brain Mapp. 2002; 16(1):47–62. [PubMed: 11870926]

Makeig S, Delorme A, Westerfield M, Jung TP, Townsend J, Courchesne E, Sejnowski TJ. Electroencephalographic brain dynamics following manually responded visual targets. PLoS Biol. 2004; 2(6):747–62.

Marinkovic K, Cox B, Reid K, Halgren E. Head position in the MEG helmet affects the sensitivity to anterior sources. Neurol Clin Neurophysiol. 2004; 2004:30. [PubMed: 16012659]

Marinkovic K, Halgren E, Maltzman I. Arousal-related P3a to novel auditory stimuli is abolished by a moderately low alcohol dose. Alcohol Alcohol. 2001; 36(6):529–39. [PubMed: 11704618]

McCarthy G, Luby M, Gore J, Goldman-Rakic P. Infrequent events transiently activate human prefrontal and parietal cortex as measured by functional MRI. J Neurophysiol. 1997; 77(3):1630–4. [PubMed: 9084626]

McCarthy G, Wood CC, Williamson PD, Spencer DD. Task-dependent field potentials in human hippocampal formation. Journal of Neuroscience. 1989; 9:4253–4268. [PubMed: 2593001]

Mecklinger A, Maess B, Opitz B, Pfeifer E, Cheyne D, Weinberg H. A MEG analysis of the P300 in visual discrimination tasks. Electroencephalogr Clin Neurophysiol. 1998; 108(1):45–56. [PubMed: 9474061]

Meijs JWH, Bosch FGC, Peters MJ, Lopes da Silva FH. On the magnetic field distribution generated by a dipolar current source situated in a realistically shaped compartment model of the head. Electroencephalography and Clinical Neurophysiology. 1987; 66:286–298. [PubMed: 2434313]

Meijs JWH, Peters MJ. The EEG and MEG, Using a model of eccentric spheres to describe the head. IEEE Transactions on Biomedical Engineering. 1987; 34:913–920. [PubMed: 3692512]

Naatanen, R. Attention and brain function. Lawrence Erlbaum Asso.; New Jersey: 1992. p. 495

Nishitani N, Ikeda A, Nagamine T, Honda M, Mikuni N, Taki W, Kimura J, Shibasaki H. The role of the hippocampus in auditory processing studied by event-related electric potentials and magnetic fields in epilepsy patients before and after temporal lobectomy. Brain. 1999; 122(Pt 4):687–707. [PubMed: 10219782]

Nishitani N, Nagamine T, Fujiwara N, Yazawa S, Shibasaki H. Cortical-hippocampal auditory processing identified by magnetoencephalography. J Cogn Neurosci. 1998; 10(2):231–47. [PubMed: 9555109]

Nordby H, Roth WT, Pfefferbaum A. Event-related potentials to breaks in sequences of alternating pitches or interstimulus intervals. Psychophysiology. 1988; 25:262–268. [PubMed: 3406327]

Okada YC, Kaufman L, Williamson SJ. The hippocampal formation as a source of the slow endogenous potentials. Electroencephalogr Clin Neurophysiol. 1983; 55(4):417–26. [PubMed: 6187535]

Onofrj M, Fulgente T, Nobilio D, Malatesta G, Bazzano S, Colamartino P, Gambi D. P3 recordings in patients with bilateral temporal lobe lesions. Neurology. 1992; 42(9):1762–7. [PubMed: 1513467]

Oostendorp, TF.; Van Oosterom, A. Source parameter estimation using realistic geometry in bioelectricity and biomagnetism. In: Nenonen, J.; Rajala, HM.; Katila, T., editors. Biomagnetic Localization and 3D Modeling. Helsinky Univ. of Technology; Helsinki: 1992. Report TKK-F-A689

Pincze Z, Lakatos P, Rajkai C, Ulbert I, Karmos G. Effect of deviant probability and interstimulus/interdeviant interval on the auditory N1 and mismatch negativity in the cat auditory cortex. Brain Res Cogn Brain Res. 2002; 13(2):249–53. [PubMed: 11958968]

Polich J, Squire LR. P300 from amnesic patients with bilateral hippocampal lesions. Electroencephalography and Clinical Neurophysiology. 1993; 86:408–417. [PubMed: 7686475]

Puce A, Kalnins RM, Berkovic SF, Donnan GA, Bladin PF. Limbic P3 potentials, seizure localization, and surgical pathology in temporal lobe epilepsy. Annals of Neurology. 1989; 26:377–385. [PubMed: 2802537]

Rektor I, Kanovsky P, Bares M, Louvel J, Lamarche M. Event-related potentials, CNV, readiness potential, and movement accompanying potential recorded from posterior thalamus in human subjects. A SEEG study. Neurophysiol Clin. 2001; 31(4):253–61. [PubMed: 11596532]

Rogers RL, Baumann SB, Papanicolaou AC, Bourbon TW, Alagarsamy S, Eisenberg HM. Localization of the P3 sources using magnetoencephalography and magnetic resonance imaging. Electroencephalogr Clin Neurophysiol. 1991; 79(4):308–21. [PubMed: 1717235]

Romanski LM, Goldman-Rakic PS. An auditory domain in primate prefrontal cortex. Nat Neurosci. 2002; 5(1):15–6. [PubMed: 11753413]

Romanski LM, Tian B, Fritz J, Mishkin M, Goldman-Rakic PS, Rauschecker JP. Dual streams of auditory afferents target multiple domains in the primate prefrontal cortex. Nat Neurosci. 1999; 2(12):1131–6. [PubMed: 10570492]

Rosburg T, Trautner P, Dietl T, Korzyukov OA, Boutros NN, Schaller C, Elger CE, Kurthen M. Subdural recordings of the mismatch negativity (MMN) in patients with focal epilepsy. Brain. 2005; 128(Pt 4):819–28. [PubMed: 15728656]

Rosburg T, Trautner P, Ludowig E, Schaller C, Kurthen M, Elger CE, Boutros NN. Hippocampal event-related potentials to tone duration deviance in a passive oddball paradigm in humans. Neuroimage. 2007; 37(1):274–81. [PubMed: 17560796]

Roth WT, Krainz PL, Ford JM, Tinklenberg JR, Rothbart RM, Kopell BS. Parameters of temporal recovery of the human auditory evoked potential. Electroencephalography and Clinical Neurophysiology. 1976; 40:623–632. [PubMed: 57048]

Scherg M, VonCramon D. Two bilateral sources of the late AEP as identified by a spatiotemporal dipole model. Electroencephalography and Clinical Neurophysiology. 1985; 62:32–44. [PubMed: 2578376]

Smith ME, Halgren E, Sokolik M, Baudena P, Musolino A, Liegeois-Chauvel C, Chauvel P. The intracranial topography of the P3 event-related potential elicited during auditory oddball. Electroencephalogr Clin Neurophysiol. 1990; 76(3):235–48. [PubMed: 1697255]

Soltani M, Knight RT. Neural origins of the P300. Crit Rev Neurobiol. 2000; 14(3–4):199–224. [PubMed: 12645958]

Squires, NK.; Halgren, E.; Wilson, CL.; Crandall, PH. Human endogenous limbic potentials: Cross-modality and depth/surface comparisons in epileptic subjects. In: Gaillard, AWK.; Ritter, W., editors. Tutorials in ERP Research: Endogenous Components. Amsterdam; North Holland: 1983. p. 217-232.

Squires NK, Squires KC, Hillyard SA. Two varieties of long-latency positive waves evoked by unpredictable auditory stimuli in man. Electroencephalography and Clinical Neurophysiology. 1975; 38(4):387–401. [PubMed: 46819]

Stapleton JM, Halgren E. Endogenous potentials evoked in simple cognitive tasks: Depth components and task correlates. Electroencephalography and Clinical Neurophysiology. 1987; 67:44–52. [PubMed: 2439280]

Tarkka IM, Stokic DS, Basile LF, Papanicolaou AC. Electric source localization of the auditory P300 agrees with magnetic source localization. Electroencephalogr Clin Neurophysiol. 1995; 96(6):538–45. [PubMed: 7489675]

Trainor LJ, McDonald KL, Alain C. Automatic and controlled processing of melodic contour and interval information measured by electrical brain activity. J Cogn Neurosci. 2002; 14(3):430–42. [PubMed: 11970802]

Velasco M, Velasco F, Velasco AL. Intracranial studies on potential generators of some vertex auditory evoked potentials in man. Stereotact Funct Neurosurg. 1989; 53(1):49–73. [PubMed: 2740657]

Verleger R. P3b: Towards some decision about memory. Clin Neurophysiol. 2008; 119:968–970. [PubMed: 18222107]

Watanabe N, Hirai N, Maehara T, Kawai K, Shimizu H, Miwakeichi F, Uchida S. The relationship between the visually evoked P300 event-related potential and gamma band oscillation in the human medial and basal temporal lobes: an electrocorticographic study. Neurosci Res. 2002; 44(4):421–7. [PubMed: 12445629]

Wilson CL, Babb TL, Halgren E, Wang ML, Crandall PH. Habituation of human limbic neuronal response to sensory stimulation. Exp Neurol. 1984; 84(1):74–97. [PubMed: 6705888]

Yingling CD, Hosobuchi Y. A subcortical correlate of P300 in man. Electroencephalography and Clinical Neurophysiology. 1984; 59:72–76. [PubMed: 6198167]

Zatorre RJ. Neural specializations for tonal processing. Ann N Y Acad Sci. 2001; 930:193–210. [PubMed: 11458830]

Zatorre RJ, Evans AC, Meyer E. Neural mechanisms underlying melodic perception and memory for pitch. J Neurosci. 1994; 14(4):1908–19. [PubMed: 8158246]

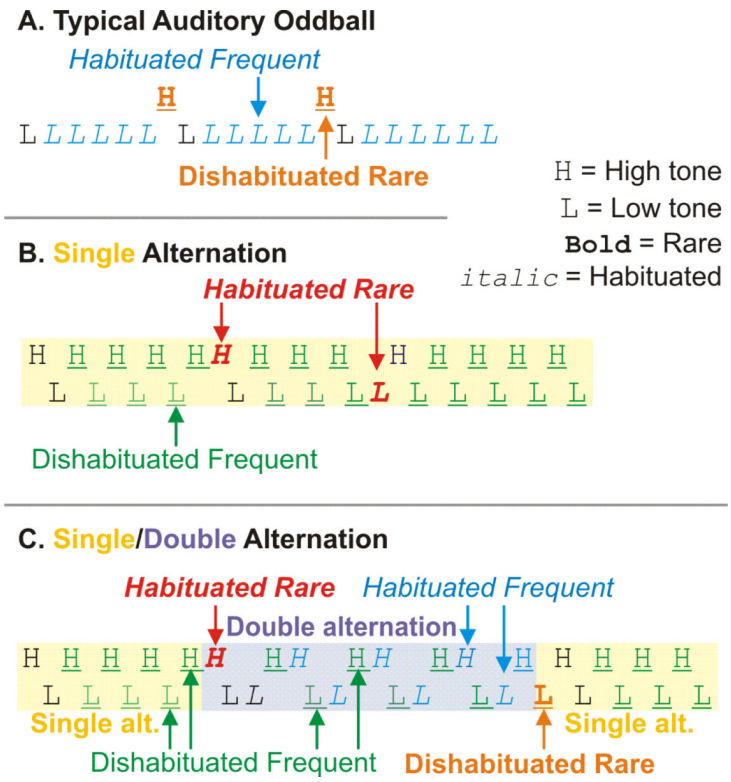


**Figure 1. Task**

In the typical Auditory Oddball task (**A**), subjects count **rare** target tones that occur randomly intermixed with frequent tones. The **rare** and frequent tones differ in pitch, and the frequent tones are *habituated* because they are preceded by identical frequent tones, whereas the rare tones are dis-habituated. In a Single Alternation task (**B**), the subject detects rare repetitions of high or low-pitched tones amongst the frequent alternation in pitch. Since the **rare** tones are identical to the preceding tone, they are *habituated*, whereas the frequent are dis-habituated. Thus, in both cases, habituation is confounded with rarity and targetness. In the Single/Double Alternation task utilized here (**C**), subjects count shifts between single- and double-alternation of high and low pitched tones. As shown in the top line, half of the tones indicating that a **rare** shift had occurred were identical in pitch to the preceding tone (*habituated*), whereas, as shown in the bottom line, half of the rares were dis-habituated. Similarly, pitch and habituation status are balanced for the frequent non-target tones.

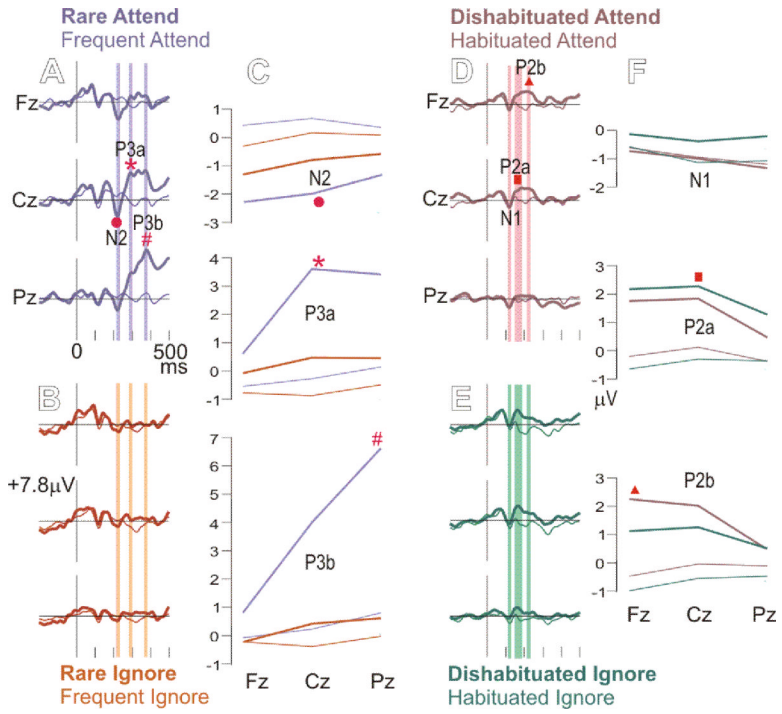


**Figure 2. Grand average ERP waveforms at midline scalp sites**

Event-Related Potentials, as recorded at the frontal (Fz), central (Cz) and parietal (Pz) scalp midline. The attended rare shifts in the tone sequence (**A**) evoked an N2 (●), P3a (✱), and P3b (#). The P3a and P3b are greatly decreased when the tones are ignored (**B**), whereas the N2 is relatively little changed. The vertical bars show the latency ranges when the average amplitudes corresponding to the N2, P3a and P3b were measured (**A**, **B**). These amplitudes are plotted in **C**, where the N2 (●) to rare shifts (thick lines) is more negative than to frequent tones (thin lines), and is little changed whether the stimuli are attended (purple) or ignored (orange). In contrast, both rarity and attention are required for the P3a (✱, thick purple) and P3b (#, thick purple). At right, waveforms evoked by frequent tones with different states of habituation are compared (**D**, **E**, **F**). The vertical bars show latency ranges for estimating the N1, P2a, and P2b (**D**, **E**). At early latency (N1 period), the frequent tones evoked a small negativity in all conditions. A positive wave at about the same latency as the N2 is larger when the tone's pitch is different from that of the immediately preceding tone (thick vs thin lines, marked with ■,▲). Similar waveforms are evoked by attended (**D**) versus ignored (**E**) frequent tones, and average amplitude measurements confirm this (green vs brown lines, panel **F**).

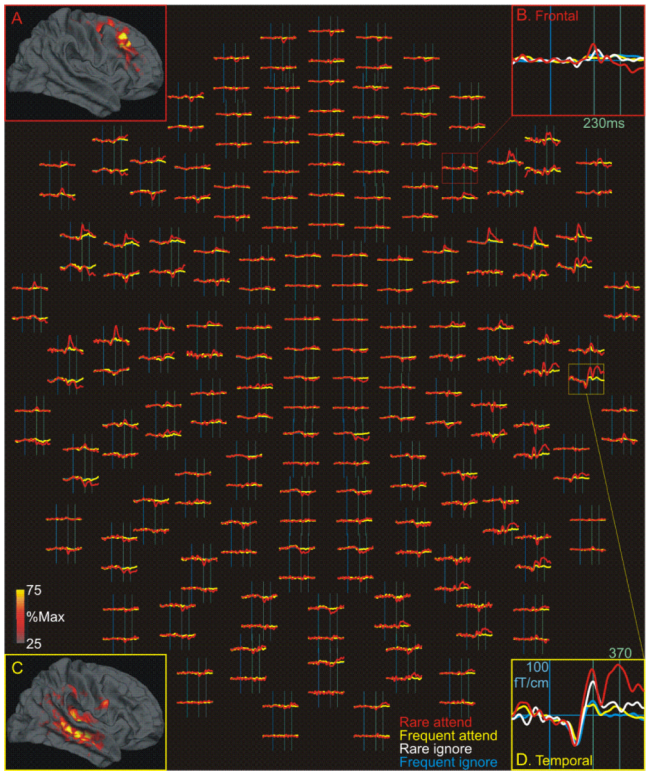


**Figure 3. Gradiometer waveforms in a typical subject**

Average responses to attended rare and frequent stimuli at all 204 gradiometers are shown in the center of the figure. Activity at single sensors over the frontal lobe (red box) and over the temporal lobe (yellow box) are expanded for clearer view (**B,D**). The lead fields for these sensors (**A,C**) were calculated as the contribution of each cortical dipole to the signal recorded at the sensor, relative to the contribution of the dipole that contributes the most. Shown here are the lead fields averaged across subjects; the individual subject lead fields are shown in figure 10. The sensor over the frontal lobe (#1233) records almost exclusively from dorsolateral prefrontal cortex (**A**), whereas the sensor over the temporal lobe (#2612) records mainly from temporal cortex with a small contribution from supramarginal and ventral precentral cortices (**C**). Note that both frontal and temporal sensors record large responses to attended rare stimuli, but with different time courses.

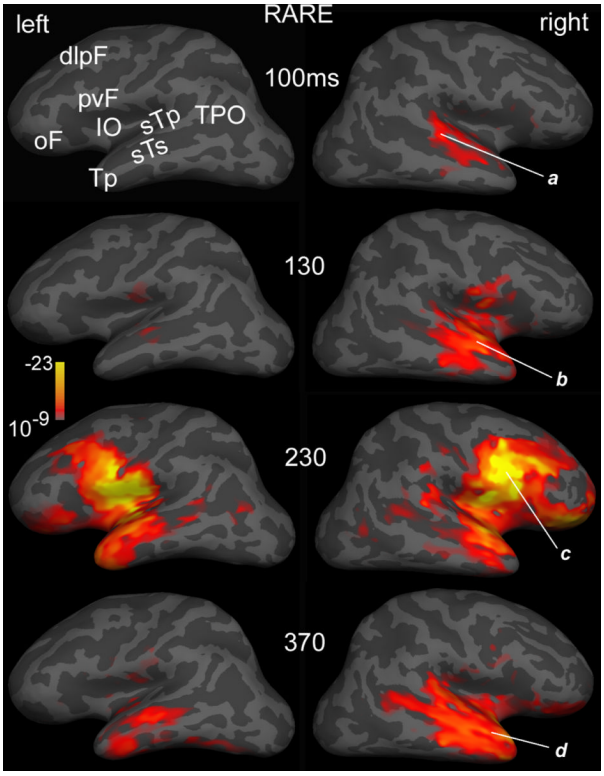


**Figure 4. Statistical parametric maps of activity evoked by attended rare tones**

Snapshots of cortical activity were estimated at 4 latencies using an anatomically-constrained noise-normalized minimum norm inverse solution. Lateral views of the left and right hemispheres are inflated so that cortical areas within the sulci (dark gray) as well as crowns (light gray) are visible. Activity in the right superior temporal plane (sTp) and superior temporal sulcus (sTs) at 100 ms (***a***) spreads to adjacent areas at 130 ms (***b***). At ~230 ms (***c***) bilateral activity is most prominent in the posteroventral frontal cortex (pvF), but is significant also in the insulo-opercular (IO), temporal pole (Tp), orbitofrontal (oF), and dorsolateral prefrontal (dlpF) cortices. The final peak, at ~370 ms (***d***), is predominantly temporal, including the Tp, sTs, sTp, and extending on the left posteriorly to the temporo-parieto-occipital (TPO) junction. Average of 8 subjects, gradiometers only. Significance is mapped, from a threshold of $p<10^{-9}$, through full red $p<10^{-13}$, to full yellow $p<10^{-23}$.

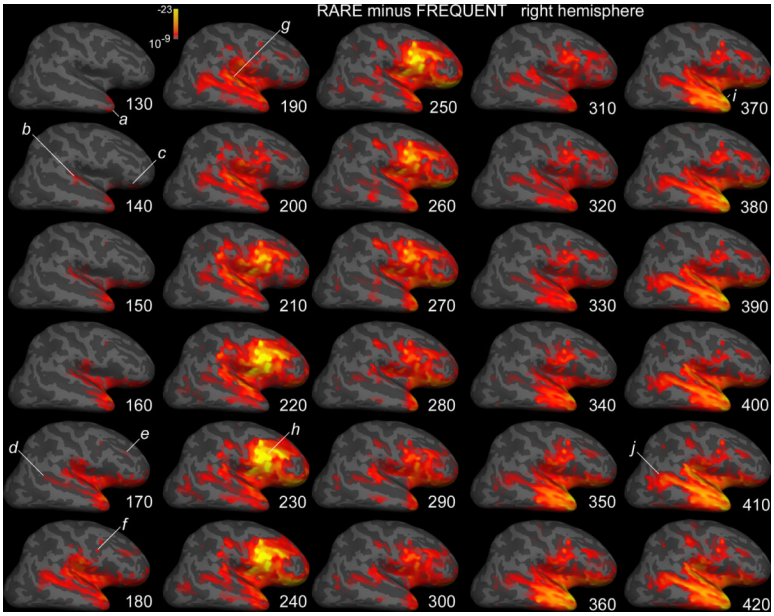


**Figure 5. Attended rare minus frequent tones**

Differential activity to rare as compared to frequent tones is estimated at 10 ms intervals from 130 through 420 ms. The cross-subject average is displayed on the inflated surface of the right hemisphere. The earliest activity, at ~130 ms in Tp (***a***), spreads by ~140 ms to sTp (***b***), oF (***c***) and IO. Activity increases in these sites and spreads to the sTs, TPO (***d***), and dlpF (***e***) by ~170 and pvF by ~180 ms (***f***). An initial peak of activity centered in sTp at ~190 ms (***g***), is followed by a peak centered in pvF at ~230 ms (***h***), and Tp at ~370 ms (***i***). At longer latencies, activity in TPO is increasingly prominent (***j***). Abbreviations as in figure 4, gradiometers only.

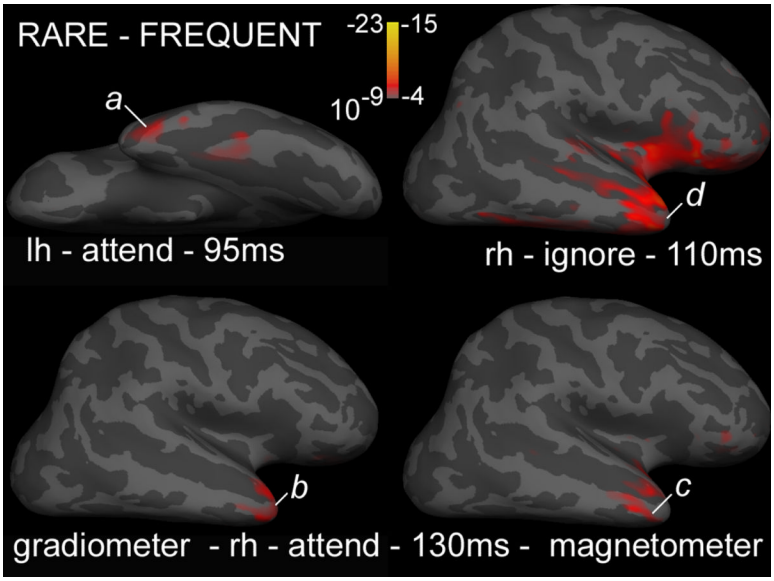


**Figure 6. Apparent onset of differential activity to rare tones in the temporal pole**

The earliest significant differential activity in the cross-subject averages to rare as compared to frequent tones is shown in a ventral view of the left hemisphere (***a***), as well as lateral views of the right hemisphere (***b,c,d***). Activity is estimated either from the gradiometers (***a,b,d***) or magnetometers (***c***). Abbreviations and scale for the attend condition (***a,b,c***) are as in figure 4, but are lowered for the ignore condition (***d***) to a threshold of $p<10^{-4}$, and full red of $p<10^{-7}$. In all cases the earliest activity arises in Tp.

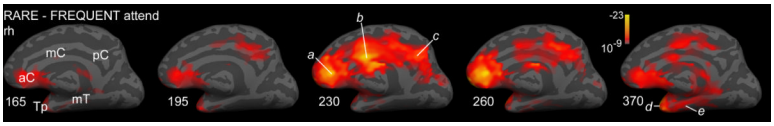


**Figure 7. Differential activity to rare tones in medial cortex**

Strongly significant differential activity to rare as compared to frequent tones is estimated to arise in the anterior cingulate cortex (aC, ***a***) in medial views of the right hemisphere at 165, 185, 230, 260, and 370 ms. Activity peaks in middle cingulate (mC, ***b***) and posterior cingulate (pC, ***c***) cortices at ~230 ms, and in Tp and medial temporal cortex (mT, ***d,e***) at ~370 ms. Cross-subject averages from gradiometer data.

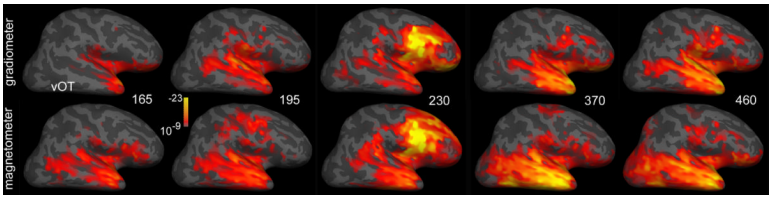


**Figure 8. Comparison of activity estimates from gradiometers versus magnetometers**

Differential activity evoked by attended rare as compared to frequent tones was estimated from the 204 gradiometers (top row) and 102 magnetometers (bottom row) Similar results were obtained. Cross-subject averages.

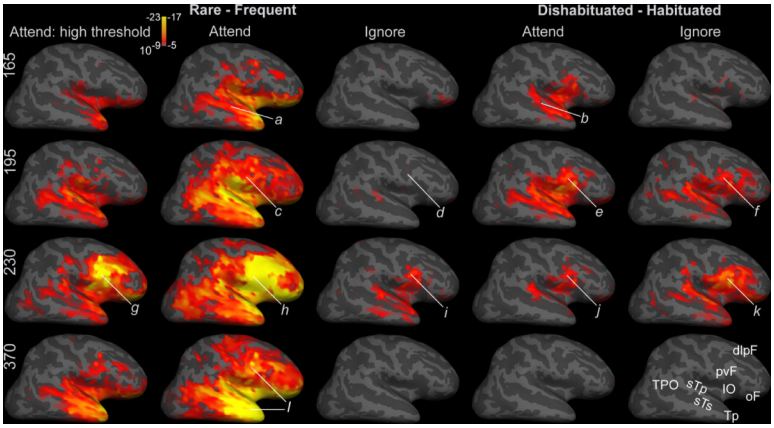


**Figure 9. Effects of rarity and dishabituation for attended and ignored conditions**

Lateral views of the right hemisphere at 4 latencies show differential activity evoked by rare as compared to frequent tones (left 3 columns), and by dishabituated as compared to habituated frequent tones (right 2 columns). At 165 ms attended rare (***a***) and attended dishabituated (***b***) tones both evoke differential activity in frontotemporal sites, with the response to rarity most significant in Tp, IO and oF, and that to dishabituation in sTp, sTs, IO and pvF. These responses increase at 195 ms (**c,e**), at which time the ignored dishabituated tones evoke differential activity in frontotemporal sites (***f***), whereas ignored rare tones do not (***d***) until ~230 ms (***i***). At this time, differential activity in pvF, IO and sTp is evoked by attended and ignored, rare and habituated tones (***g,h,i,j,k***). Note that at both 195 and 230 ms, more differential activity is evoked by ignored dishabituated tones (***f,k***) than by ignored rare tones (***d,i***). However, at longer latencies, differential activity was only evoked by attended rare tones (***l***). Since more differential activity was evoked by rare attended tones than the other conditions, it is plotted with two significance scales. Significance scales in the left column are as in figure 4, but are lower in the other columns, with a threshold of $p<10^{-5}$, full red indicating $p<10^{-8}$, and full yellow $p<10^{-17}$. The high threshold at left allows the anatomical distribution of activity to be better appreciated, whereas the consistent threshold at right allows activity levels to be compared across conditions. Abbreviations for the cortical areas in the lower right brain are as in figure 4. Cross-subject averages from gradiometer data.

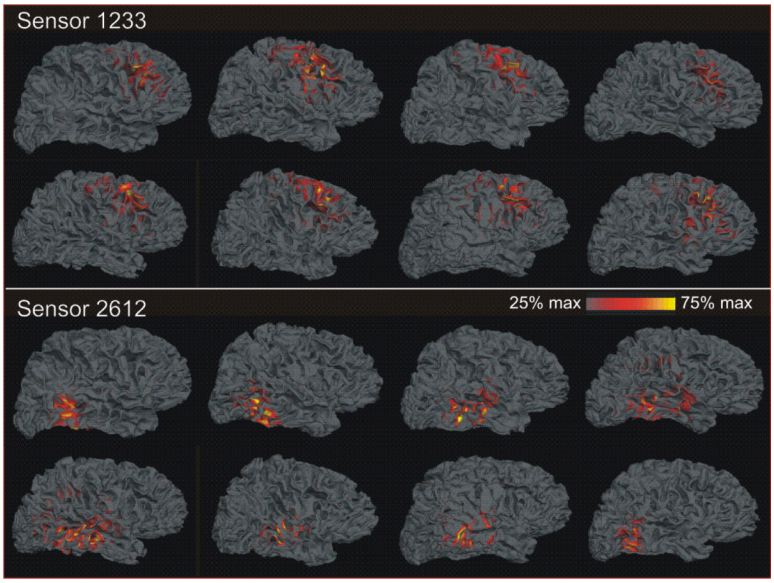


**Figure 10. Cortical lead fields for the sensors used for statistical analysis**

The lead fields for these sensors were calculated in each of the eight subjects as the contribution of each cortical dipole to the signal recorded at the sensor, relative to that of the dipole that contributes the most to that sensor. Please see Figure 3 for these lead fields averaged across subjects after aligning the sulcal gyral patterns of the individual brains. The lead field plots show that the selected sensor #1233 records from a consistent area of the posterior dorsolateral prefrontal cortex in each subject, whereas the other selected sensor #2612 records from superior and middle temporal gyri in all subjects, with occasional small contributions from immediately adjacent areas.